Low-Carbon Unit Commitment with Pumped Storage Hydropower under High Solar PV Penetration Using Mixed-Integer Nonlinear Programming

Ramdhan Halid Siregar
Department of Electrical and Computer Engineering, Universitas Syiah Kuala, Banda Aceh, Indonesia
ramdhan@usk.ac.id (corresponding author)

Rakhmad Syafutra Lubis
Department of Electrical and Computer Engineering, Universitas Syiah Kuala, Banda Aceh, Indonesia
rakhmadslubis@usk.ac.id

Akhyar
Department of Mechanical and Industrial Engineering, Universitas Syiah Kuala, Banda Aceh, Indonesia
akhyar@usk.ac.id

Muhammad Nurul Hadi
Department of Electrical and Computer Engineering, Universitas Syiah Kuala, Banda Aceh, Indonesia
mnurulhadi74@gmail.com

Received: 16 March 2026 | Revised: 2 April 2026 and 22 April 2026 | Accepted: 23 April 2026

 DOI: https://doi.org/10.48084/etasr.18785

ABSTRACT

High Photovoltaic (PV) penetration introduces operational challenges in power systems, particularly the duck curve phenomenon, which increases ramping requirements for thermal generators. This study proposes a low-carbon Unit Commitment (UC) model formulated as a Mixed Integer Nonlinear Programming (MINLP) problem integrating Pumped Storage Hydropower (PSH). The objective function simultaneously considers fuel cost, startup cost, and carbon emission cost. The model is implemented in Python and solved using the SCIP solver over a 24-hour scheduling horizon for a system consisting of ten thermal units, four PV farms, and four PSH units. Simulation results show that the baseline scenario results in a total operating cost of $342,083.98 with carbon emissions of 172.02 t. The integration of PSH reduces the operating cost to $334,436.20 but slightly increases emissions to 176.09 t. When carbon-aware optimization is combined with PSH, the total cost becomes $336,102.74 with emissions of 173.60 t. Although the proposed approach does not significantly reduce total emissions compared to the baseline, it improves economic performance and smooths net-load fluctuations, thereby enhancing operational flexibility. These results indicate that integrating PSH within a carbon-aware UC framework provides a more balanced trade-off between cost and emission considerations in PV-dominated power systems.

Keywords-carbon emission; distributed generation; duck curve; Mixed Integer Nonlinear Programming (MINLP); Pumped Storage Hydropower (PSH); Photovoltaic (PV); Unit Commitment (UC)

I. INTRODUCTION

Photovoltaic (PV) technology has become one of the fastest-growing renewable energy sources due to its decreasing installation cost and improving efficiency [1-3]. The increasing penetration of PV generation plays a crucial role in supporting the transition toward low-carbon and sustainable energy systems [4-7]. However, the inherent variability and intermittency of PV output introduce significant operational challenges in maintaining the balance between electricity supply and demand [8-11].

One of the most critical issues associated with high PV penetration is the duck curve phenomenon, which is characterized by a substantial reduction in net load during daytime followed by a steep ramping requirement in the

evening [12-16]. This condition imposes considerable stress on thermal power plants, as they must frequently adjust their output despite operational constraints such as ramp limits and minimum up/down times [9, 17]. Consequently, system operation becomes less efficient and may lead to increased fuel consumption and carbon emissions [18-21].

To address these challenges, various solutions have been proposed in the literature. Energy Storage Systems (ESS), particularly Pumped Storage Hydropower (PSH), are widely recognized as effective technologies for mitigating net load fluctuations due to their large capacity, fast response, and high reliability [14, 22-27]. In addition, advanced forecasting and demand-side management strategies have also been explored to reduce the severity of the duck curve [13, 28].

On the other hand, Unit Commitment (UC) optimization has been extensively studied to determine the optimal scheduling of generation units while minimizing operational costs under system constraints [29-32]. More recently, environmental concerns have led to the development of low-carbon UC models, which incorporate carbon emission costs into the optimization framework to support sustainable power system operation [33, 34].

Despite these advancements, most existing studies focus on individual aspects such as economic optimization [29-32], energy storage integration [23-27], or emission-aware UC [33, 34], which are typically investigated separately. The combined impact of integrating PSH and carbon-aware UC within a unified optimization framework remains insufficiently explored, particularly under high PV penetration conditions. Furthermore, the trade-off between economic performance and carbon emissions in such integrated systems is still not well understood.

Therefore, this study proposes a low-carbon UC model formulated as a Mixed Integer Nonlinear Programming (MINLP) problem, integrating PSH to mitigate the operational challenges caused by the duck curve. The proposed model simultaneously considers fuel cost, startup cost, and carbon emission cost within a unified optimization framework.

Unlike previous studies, this work integrates economic, environmental, and flexibility aspects into a single framework under high PV penetration. In addition, it provides a comprehensive analysis of the interaction between PSH operation and carbon-aware scheduling, particularly in terms of system flexibility and generator dispatch.

The study also evaluates the trade-off between operating cost and carbon emissions across multiple scenarios, offering deeper insights into system performance in PV-dominated power systems.

II. METHODOLOGY

The resolution of the duck curve problem begins with the collection of generation unit characteristics and load demand data. Subsequently, a mathematical model of the system is constructed based on the available data. This model must be formulated in a form that can be solved using MINLP. To simplify the model and reduce the computational burden, power flow analysis is not included in the formulation. Once the modeling process is completed, the problem is solved using an MINLP solver. In this study, the SCIP software was employed through the Python programming language.

A. Unit Commitment Modeling

One of the main aspects in applying the MINLP method to a problem is formulating the system into a mathematical representation that can be effectively handled by the solver. In general, the UC model can be divided into two main components, namely the objective function and the constraint model. The formulation adopted in this study is adapted from established UC models and system configurations reported in previous studies [35, 36].

The optimization process of UC is closely related to Economic Dispatch (ED), which determines the optimal power output of committed generators in order to minimize the total operating cost at each time period. In performing UC and ED optimization, two main approaches are commonly used. Authors in [25] conducted UC optimization first, followed by ED optimization, whereas authors in [29] performed UC and ED simultaneously within a unified framework.

In this study, the ED process is carried out simultaneously with UC. This integrated approach ensures that the total operating cost of the generators is optimally minimized while satisfying all operational constraints. However, this formulation increases the computational complexity of the problem. To address this issue, the optimization model is solved using the SCIP solver, which is capable of handling large-scale MINLP problems efficiently.

1) Unit Commitment Objective Function

In the UC problem, the objective function is the minimization of the total generation cost of the system. The formulation used in this study follows conventional UC models reported in the literature [34, 35]. Two types of generation costs are considered: the operational costs of thermal generators and the operational costs of the PSH. The operational costs of thermal generators include startup costs and fuel costs. For the PSH, costs arise from its operation and maintenance.

- Objective function of UC:

$$\min F = \sum_{t=1}^{N_T} \left\{ \sum_{i=1}^{N_G} \left[FC_i \left(P_{GT_i}(t) \right) + CC_i(t) \right] + SDC(t) + SUC(t) + \sum_{i=1}^{N_{PSH}} C_{PSH_i}(t) \right\} \quad (1)$$

where F is the total operating cost ($), N_T is the scheduling horizon (h), N_G is the number of thermal generators, N_{PSH} is the number of PSH units, $FC_i \left(P_{GT_i}(t) \right)$ is the fuel cost of generator i at time t, $SUC(t)$ is the startup cost, $SDC(t)$ is the shutdown cost, and $C_{PSH_i}(t)$ is the operational cost of PSH unit i.

- Fuel cost function of thermal generators:

$$FC_i \left(P_{GT_i}(t) \right) = a_i + b_i P_{GT_i}(t) + c_i P_{GT_i}^2(t) \quad (2)$$

where a_i , b_i , and c_i are the fuel cost coefficients of generator i, and $P_{GT_i}(t)$ is the power output (MW).

- Carbon cost function of thermal generators:

$$CE_i\left(P_{GT_i}(t)\right) = \left(\alpha_i + \beta_i P_{GT_i}(t) + \gamma_i P_{GT_i}^2(t)\right) * 0.01 + \omega_i e^{\mu_i P_{GT_i}(t)} \quad (3)$$

$$CC_i = CE_i \cdot CE_{tax} \quad (4)$$

where $CE_i\left(P_{GT_i}(t)\right)$ is the carbon emission of thermal generator i at time t (t), $P_{GT_i}(t)$ is the power output of generator i at time t (MW), α_i , β_i , and γ_i are the polynomial emission coefficients, ω_i and μ_i are the exponential emission coefficients, and CE_{tax} is the carbon tax (\$/t). $CC_i(t)$ represents the carbon emission cost of generator i at time t (\$).

- Startup cost model of thermal generators:

$$SUC(t) = \sum_{i=1}^{N_{TG}} SUC_i(u_{i,t} - u_{i,t-1})\ u_{i,t} \quad (5)$$

where SUC_i is the startup cost of generator i, and $u_{i,t}$ is the on/off status (1 if ON, 0 if OFF).

- Shutdown cost model of thermal generators:

$$SDC(t) = \sum_{i=1}^{N_{TG}} SDC_i(u_{i,t-1} - u_{i,t})\ u_{i,t-1} \quad (6)$$

where SDC_i is the shutdown cost of generator i.

- Operational cost model of PSH

$$C_{PSH_i}(t) = P_{PSH_i}^{out}(t) \cdot O_{PSH_i} \quad (7)$$

where $C_{PSH_i}(t)$ is the operational cost of PSH unit i at time t (\$), $P_{PSH_i}^{out}(t)$ is the output (discharging) power of PSH unit i at time t (MW), and O_{PSH_i} is the operational cost coefficient of PSH unit i (\$/MWh).

2) Unit Commitment Constraint Model

There are several constraints that must be satisfied in the optimization of UC. These constraints can be categorized into three groups: power balance constraints, thermal generator constraints, and PSH operation constraints. The power balance constraint requires that the total load must be equal to the total power generated in each period. Thermal generator constraints are defined based on the specifications of each thermal unit. Meanwhile, the PSH constraints are determined according to the technical specifications of the PSH system used.

- Power balance constraint model:

$$P_{LD}(t) = \sum_{i=1}^{N_{TG}} P_{GT_i}(t) + \sum_{j=1}^{N_{PV}} P_{PV_j}(t) + \sum_{k=1}^{N_{PSH}} P_{PSH_k}^{out}(t) - \sum_{k=1}^{N_{PSH}} P_{PSH_k}^{in}(t) \quad (8)$$

where $P_{LD}(t)$ is the load demand at time t (MW), N_{TG} , N_{PV}, and N_{PSH} represent the number of thermal generators, PV units, and PSH units, respectively. $P_{GT_i}(t)$ is the power output of thermal generator i, $P_{PV_j}(t)$ is the power output of PV unit j, $P_{PSH_k}^{out}(t)$ is the discharging power of PSH unit k, and $P_{PSH_k}^{in}(t)$ is the charging power of PSH unit k.

- Thermal generator power output constraint:

$$P_{GT_i}^{min} \le P_{GT_i} \le P_{GT_i}^{max} \quad (9)$$

where $P_{GT_i}^{min}$ is the minimum power output and $P_{GT_i}^{max}$ is the maximum power output of generator i.

- Thermal generator minimum up-time constraint:

$$MUT_i\ u_{i,t}\left(u_{i,t} - u_{i,t-1}\right) = \sum_{t=1}^{t=MUT_i} u_{i,t} \quad (10)$$

where MUT_i is the generator minimum up-time.

- Thermal generator minimum down-time constraint:

$$MDT_i u_{i,t-1}\left(u_{i,t-1} - u_{i,t}\right) = \sum_{t=1}^{t=MDT_i} u_{i,t} \quad (11)$$

where MDT_i is the generator minimum down-time.

- PSH capacity constraint model:

$$E_{PSH_i}(t) = E_{PSH_i}(t-1) + \eta_{ch} P_{PSH_i}^{in}(t) - \eta_{dis} P_{PSH_i}^{out}(t) \quad (12)$$

where $E_{PSH_i}(t)$ is the stored energy of PSH unit i at time t (MWh), $E_{PSH_i}(t-1)$ is the stored energy at the previous time step, $P_{PSH_i}^{in}(t)$ is the charging power, and $P_{PSH_i}^{out}(t)$ is the discharging power (MW). η_{ch} and η_{dis} denote the charging and discharging efficiencies, respectively.

B. Algorithm Flow

In this study, the Python programming language was employed to facilitate the optimization of UC. Python was chosen because MINLP solvers are readily available within the programming environment, thereby enabling a more straightforward implementation of the optimization program.

Based on Figure 1, it can be observed that the UC optimization program begins with the initialization of the input data. The program then generates a set of variables corresponding to the available data. These variables are subsequently formulated into an MINLP model to be optimized. The SCIP solver is then called to optimize the MINLP UC model. If SCIP successfully executes the model, the program exports the optimization results into an Excel file. However, if an error occurs in the constructed model, SCIP will display an error message. Such errors generally arise when the formulated model is excessively complex, making it computationally challenging and requiring an impractically long time to solve.

III. RESULTS AND DISCUSSION

A. Simulation Setup

The test system used in this study consists of ten thermal generators, four PV farms, and four PSH units. The selection of this system configuration is based on benchmark systems commonly used in previous studies. Specifically, the system structure, including the number of generators, PV units, and PSH units, as well as their operational characteristics, is adopted from [35], which provides a representative framework for analyzing the impact of high PV penetration and energy storage integration.

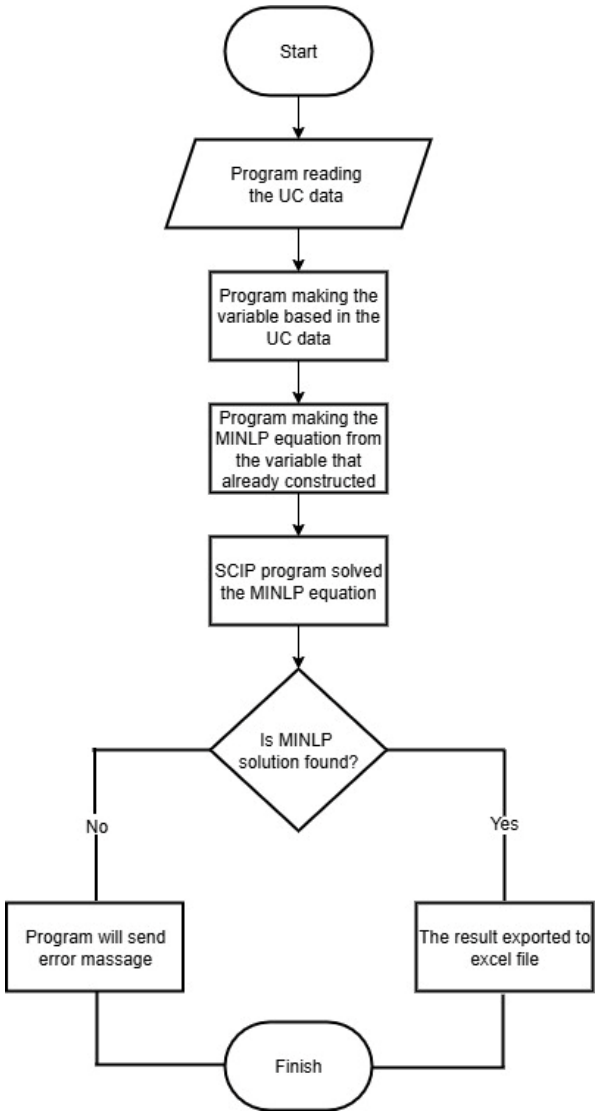

Fig. 1. Flowchart of the low-carbon UC optimization program based on the SCIP solver.

In addition, the carbon emission-related parameters of thermal generators are incorporated based on [35], since the original system in [36] does not consider emission modeling. This combination allows the proposed model to extend the benchmark system by integrating carbon-aware optimization while maintaining a realistic and widely accepted system configuration.

The simulation horizon is 24 h with hourly resolution. Figure 2 illustrates the configuration of the test system used in this study, where thermal generators (G), PV farms, PSH units, and load demand (L) are connected to the main power grid and coordinated through a unified UC framework.

The characteristics of the thermal generators and PSH units are summarized in Tables I and II. These parameters include generator operating limits, cost coefficients, and PSH storage specifications used in the optimization model.

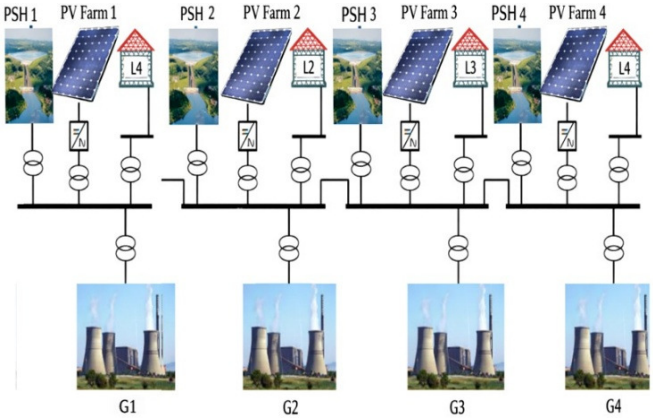

Fig. 2. Configuration of the test system used in this study.

Table I presents the fuel cost coefficients and carbon emission coefficients of the thermal generators used in this study. The coefficients a, b, and c correspond to the quadratic fuel cost function, where a represents the constant cost component, b represents the linear cost coefficient, and c represents the quadratic cost coefficient associated with generator output.

The carbon emission characteristics of each generator are modeled using coefficients α, β, and γ, which define the polynomial relationship between power output and emission levels. In addition, the parameters ω and μ are used to capture the nonlinear exponential behavior of emissions, particularly at higher generation levels. The startup cost represents the fixed cost incurred when a generator is turned on.

These parameters collectively determine both the economic and environmental performance of each generator and are used in the optimization process to evaluate the trade-off between fuel cost and carbon emission cost.

TABLE I. GENERATOR COST AND CARBON COEFFICIENTS

Unit	a ($/h)	b ($/MWh)	c ($/MW²h)	α	β	γ	ω	μ	Startup ($)
1	450	19.17	0.00398	3.9	−5.2	5.8	3.5E−4	0.3	1,800
2	665	27.17	0.00068	5.3	−4.1	4.1	7.0E−4	0.5	250
3	670	27.79	0.00064	5.5	−4.0	4.1	7.5E−4	0.6	250
4	700	16.6	0.00083	3.4	−5.6	6.1	2.8E−4	0.2	250
5	370	22.26	0.00079	4.1	−4.9	5.3	4.0E−4	0.4	520
6	480	27.24	0.002	5.8	−3.8	3.6	1.1E−3	0.7	1,100
7	680	16.5	0.00085	3.3	−5.7	6.2	2.5E−4	0.2	450
8	480	27.24	0.00098	5.1	−4.2	4.3	8.0E−4	0.5	520
9	660	25.92	0.0022	6.0	−3.7	3.5	1.5E−3	0.8	200
10	460	26.92	0.00291	6.2	−3.5	3.3	2.0E−3	0.8	200

Table II presents the operational constraints of the thermal generators, including minimum and maximum power limits, as well as minimum up-time and down-time requirements. The minimum and maximum power limits define the feasible operating range of each generator, ensuring that the output remains within technical limits.

The minimum up-time and down-time constraints are essential to represent the physical and operational limitations of thermal units, preventing frequent switching that may cause

mechanical stress and increased operational costs. These constraints play a critical role in maintaining system stability and ensuring realistic generator scheduling within the UC framework.

TABLE II. GENERATOR OPERATIONAL CONSTRAINTS

Unit	Pmin (MW)	Pmax (MW)	Minimum up-time (h)	Minimum down-time (h)
1	25	162	6	6
2	10	55	1	1
3	10	55	1	1
4	10	55	1	1
5	25	85	3	3
6	20	130	5	5
7	15	80	4	4
8	25	75	1	1
9	10	55	1	1
10	10	55	1	1

Table III summarizes the operational parameters of the PSH units. The maximum power output and storage capacity define the energy exchange capability of each unit, whereas efficiency represents the conversion performance between pumping and generating modes. The minimum up-time and down-time constraints ensure realistic operation, and the operational cost reflects the cost of PSH usage. These parameters enable PSH to perform energy shifting, helping to reduce net load fluctuations.

TABLE III. PSH PARAMETERS

Parameter	PSH 1	PSH 2	PSH 3	PSH 4
PSH maximum power output (MW)	60	48	48	36
PSH maximum capacity (MWh)	518	415	415	311
Efficiency (%)	85	85	85	85
Minimum down-time (h)	1	1	1	1
Minimum up-time (h)	1	1	1	1
Operational cost ($)	0.1	0.1	0.1	0.1

Figure 3 presents the daily PV generation and load demand profiles used in the simulation, along with the resulting net load.

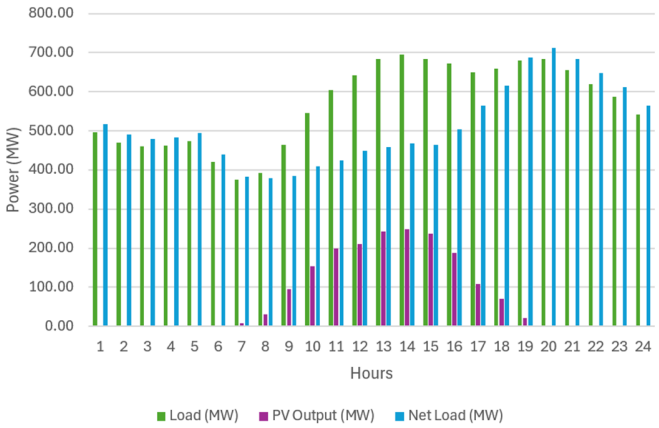

Fig. 3. Daily PV generation and load demand profiles.

As shown in Figure 3, the PV output follows a typical solar generation pattern, starting from zero in the early hours, increasing to its peak around midday, and then decreasing toward zero in the evening. In contrast, the load demand remains relatively moderate during the day and increases significantly during the evening peak period.

As a result, the net load is substantially reduced during midday due to high PV generation and increases sharply in the evening when PV output declines. This behavior forms the characteristic duck curve pattern, which introduces steep ramping requirements for thermal generators and poses operational challenges in power systems with high PV penetration.

B. Conventional Unit Commitment

In the first scenario, the UC problem is solved without considering carbon emissions in the objective function. The optimization therefore focuses on minimizing fuel cost and startup cost while satisfying generator operational constraints. The resulting generator dispatch together with the net load profile is illustrated in Figure 4.

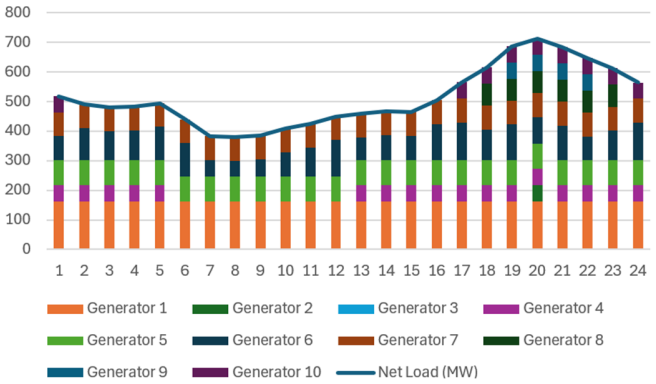

Fig. 4. Net load and thermal generator dispatch under conventional UC.

From Figure 4, it can be observed that Generator 1 operates continuously at its maximum output of 162 MW throughout the entire 24-hour period, indicating its role as the primary base-load unit. Similarly, Generator 5 and Generator 7 remain online for most of the simulation horizon, providing relatively stable outputs of approximately 85 MW and 80 MW, respectively.

Generator 6 functions as a load-following unit, adjusting its output according to system demand. Its generation varies between approximately 51.94 MW and 127.91 MW, compensating for the fluctuations in net load.

During low-demand periods, particularly between hours 6 and 12, several generators such as Generator 4, Generator 8, Generator 9, and Generator 10 remain offline. This indicates that the optimization prioritizes low-cost generators while avoiding unnecessary startup costs during off-peak periods.

As the net load increases during the evening peak period, additional generators are gradually committed. Generator 10 begins operating at hour 17, followed by Generator 8 at hour 18, and Generator 9 at hour 19. At the highest demand level

(712.98 MW at hour 20), Generator 2 is also committed to provide additional generation capacity.

The combined dispatch pattern shown in Figure 4 clearly demonstrates how the thermal generators respond to variations in net load throughout the day. The system relies on base-load units for continuous supply, whereas additional units are committed only when demand increases.

The simulation results indicate that the total thermal generation cost reaches $338,643, whereas the total carbon emissions amount to 172.02 t over the 24-hour period. Since carbon emissions are not included in the optimization objective in this scenario, the generator scheduling is determined purely by economic considerations, prioritizing cost minimization rather than emission reduction.

C. Conventional Unit Commitment with Pumped Storage Hydropower

In the second scenario, PSH is integrated into the system, whereas carbon emission costs are not included in the objective function. However, carbon emissions are still calculated and reported as performance indicators. The optimization therefore still focuses on minimizing fuel cost and startup cost, but the presence of PSH introduces additional operational flexibility in the system.

The resulting generator dispatch together with the net load profile under PSH integration is illustrated in Figure 5.

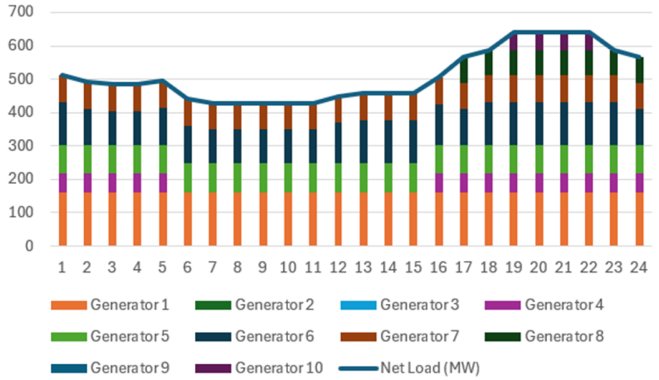

Fig. 5. Net load and thermal generator dispatch under conventional UC with PSH.

As shown in Figure 5, Generator 1 continues to operate as the main base-load unit, maintaining a constant output of 162 MW throughout the 24-hour period. Generators 5 and 7 also remain online for most of the simulation horizon, providing relatively stable outputs of approximately 85 MW and 80 MW, respectively.

Generator 6 plays a key role as a load-following unit, adjusting its output according to variations in net load. Its generation ranges from approximately 102.19 MW to 130 MW, which is noticeably smoother compared to the conventional UC case without PSH.

During low-demand periods, particularly between hours 6 and 12, several generators such as Generator 4, Generator 8, Generator 9, and Generator 10 remain offline. This indicates that the system is able to maintain supply using fewer generators due to the additional flexibility provided by PSH.

As demand increases in the evening period, additional generators are gradually committed. Generator 8 begins operating at hour 17, whereas Generator 10 is committed from hour 19 onward to support higher load levels. Compared to the previous scenario without PSH, the dispatch pattern becomes more stable and fewer abrupt generator activations are required.

To further evaluate the impact of PSH on system operation, Figure 6 compares the net load profiles between the scenarios without PSH and with PSH.

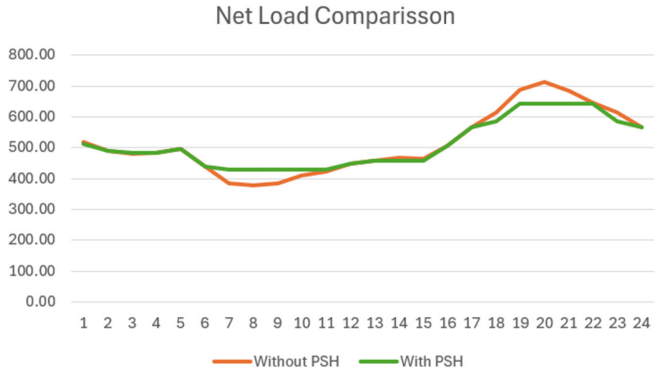

Fig. 6. Net load comparison between scenarios without PSH and with PSH.

From Figure 6, it can be observed that the integration of PSH significantly modifies the net load profile. During periods of high PV generation, PSH absorbs excess energy by operating in charging mode, which increases the net load values compared to the case without PSH. For example, the minimum net load increases from approximately 378.94 MW to around 429 MW, indicating that surplus energy is effectively stored rather than causing deep net load valleys.

During peak demand periods, PSH discharges stored energy to support the system load. As a result, the peak net load is reduced from 712.98 MW in the case without PSH to approximately 642 MW when PSH is integrated. This demonstrates that PSH effectively mitigates the steep ramping requirement associated with the duck curve phenomenon.

Overall, the integration of PSH leads to a smoother net load profile and a more stable generator dispatch schedule. The total operating cost decreases to $331,243, representing a reduction of approximately 2.2% compared to the conventional UC case without PSH. However, due to storage efficiency losses and modified generator dispatch patterns, the total carbon emissions increase slightly to 176.09 t.

D. Low-Carbon Unit Commitment

In the low-carbon UC scenario, carbon emissions are explicitly incorporated into the objective function through emission-based cost modeling. This allows the optimization process to simultaneously minimize fuel cost, startup cost, and

carbon emission cost. The performance of all simulation scenarios is summarized in Table IV, followed by the results presented in Figures 7 and 8.

TABLE IV. PERFORMANCE OF ALL SIMULATION SCENARIOS

Case	Carbon optimization	PSH	Carbon emissions (t)	Total cost ($)
Scenario I	No	No	172.02	342,083.98
Scenario II	No	Yes	176.09	334,436.20
Scenario III	Yes	No	172.02	342,083.98
Scenario IV	Yes	Yes	173.60	336,102.74

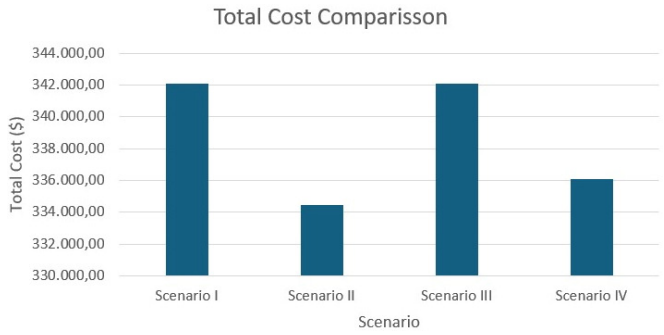

Fig. 7. Total operating cost comparison across all scenarios.

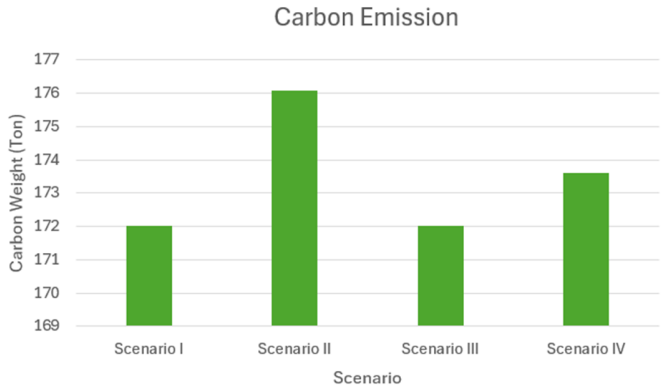

Fig. 8. Carbon emissions comparison across all scenarios.

As illustrated in Figures 7 and 8, Scenario I represents the baseline case where neither carbon optimization nor PSH is applied, resulting in a total operating cost of $342,083.98 and carbon emissions of 172.02 t. When PSH is integrated without carbon optimization (Scenario II), the total operating cost decreases significantly to $334,436.20, demonstrating the economic benefit of PSH. However, carbon emissions increase to 176.09 t due to changes in generator dispatch and storage losses.

In Scenario III, where carbon optimization is applied without PSH, both the total cost ($342,083.98) and emissions (172.02 t) remain nearly identical to the baseline case. This indicates that carbon-aware optimization alone has limited impact in the absence of additional system flexibility.

Scenario IV, which combines PSH and carbon optimization, achieves a more balanced performance. The total operating cost is reduced to $336,102.74, whereas carbon emissions decrease to 173.60 t compared to Scenario II. This demonstrates that integrating PSH with carbon-aware optimization improves the trade-off between economic performance and emission reduction in systems with high PV penetration.

IV. CONCLUSION

This study proposed a low-carbon Unit Commitment (UC) framework integrating Pumped Storage Hydropower (PSH) to address operational challenges in power systems with high Photovoltaic (PV) penetration. The optimization model was formulated as a Mixed Integer Nonlinear Programming (MINLP) problem and solved using the SCIP solver.

Four simulation scenarios were evaluated to analyze the impact of PSH integration and carbon-aware optimization. In the baseline scenario (Scenario I), the total operating cost was $342,083.98 with carbon emissions of 172.02 t. When PSH was integrated without carbon optimization (Scenario II), the operating cost decreased significantly to $334,436.20, although carbon emissions increased to 176.09 t. In Scenario III, where carbon optimization was applied without PSH, both cost and emissions remained unchanged compared to the baseline, indicating limited effectiveness due to insufficient system flexibility.

The combined approach in Scenario IV, which integrates PSH and carbon-aware optimization, resulted in a total cost of $336,102.74 and carbon emissions of 173.60 t. This scenario demonstrates a more balanced trade-off between economic performance and emission reduction compared to other scenarios.

Overall, the results indicate that while PSH effectively reduces operating costs, it may lead to a slight increase in emissions. However, when combined with carbon-aware optimization, PSH enables a more efficient and environmentally balanced system operation. Therefore, the integration of energy storage within a carbon-aware UC framework provides a promising solution for managing the challenges of high PV penetration.

DECLARATION OF COMPETING INTERESTS

The authors declare that they have no known competing financial interests or personal relationships that could have appeared to influence the work reported in this paper.

ACKNOWLEDGMENT

This research received no external funding.

DATA AVAILABILITY

The data supporting the findings of this study are available from the corresponding author upon reasonable request.

AI USE AND DECLARATION OF GENERATIVE AI USE

During the preparation of this work, the authors used ChatGPT to improve language readability and grammar. After using this tool, the authors reviewed and edited the content as needed and take full responsibility for the content of the publication.

REFERENCES

[1] A. Hassan *et al.*, "Thermal management and uniform temperature regulation of photovoltaic modules using hybrid phase change materials-nanofluids system," *Renewable Energy*, vol. 145, pp. 282–293, Jan. 2020, https://doi.org/10.1016/j.renene.2019.05.130.

[2] M. A. Fazal and S. Rubaiee, "Progress of PV cell technology: Feasibility of building materials, cost, performance, and stability," *Solar Energy*, vol. 258, pp. 203–219, July 2023, https://doi.org/10.1016/j.solener.2023.04.066.

[3] M. A. J. Al-Ani, M. A. Zdiri, F. B. Salem, and N. Derbel, "Optimized Grid-Connected Hybrid Renewable Energy Power Generation: A Comprehensive Analysis of Photovoltaic, Wind, and Fuel Cell Systems," *Engineering, Technology & Applied Science Research*, vol. 14, no. 3, pp. 13929–13936, June 2024, https://doi.org/10.48084/etasr.6936.

[4] Y. Zhao, "A Review of Renewable Energy and Power System Integration," *Applied and Computational Engineering*, vol. 126, pp. 10–15, Jan. 2025, https://doi.org/10.54254/2755-2721/2025.20092.

[5] T. Falope, L. Lao, D. Hanak, and D. Huo, "Hybrid energy system integration and management for solar energy: A review," *Energy Conversion and Management: X*, vol. 21, Jan. 2024, Art. no. 100527, https://doi.org/10.1016/j.ecmx.2024.100527.

[6] M. A. Bagherian and K. Mehranzamir, "A comprehensive review on renewable energy integration for combined heat and power production," *Energy Conversion and Management*, vol. 224, Nov. 2020, Art. no. 113454, https://doi.org/10.1016/j.enconman.2020.113454.

[7] J. Y. Lee, R. Verayiah, K. H. Ong, A. K. Ramasamy, and M. B. Marsadek, "Distributed Generation: A Review on Current Energy Status, Grid-Interconnected PQ Issues, and Implementation Constraints of DG in Malaysia," *Energies*, vol. 13, no. 24, Dec. 2020, Art. no. 6479, https://doi.org/10.3390/en13246479.

[8] E. E. Che, K. R. Abeng, C. D. Iweh, G. J. Tsekouras, and A. Fopah-Lele, "The Impact of Integrating Variable Renewable Energy Sources into Grid-Connected Power Systems: Challenges, Mitigation Strategies, and Prospects," *Energies*, vol. 18, no. 3, Feb. 2025, Art. no. 689, https://doi.org/10.3390/en18030689.

[9] M. Kammoun and M. Bourogaoui, "Future-ready power grids: From variability to predictability with scalable AI for PV energy integration," *Renewable Energy Focus*, vol. 55, Dec. 2025, Art. no. 100721, https://doi.org/10.1016/j.ref.2025.100721.

[10] P. Iliadis, S. Ntomalis, K. Atsonios, A. Nesiadis, N. Nikolopoulos, and P. Grammelis, "Energy management and techno-economic assessment of a predictive battery storage system applying a load levelling operational strategy in island systems," *International Journal of Energy Research*, vol. 45, no. 2, pp. 2709–2727, 2021, https://doi.org/10.1002/er.5963.

[11] D. Watari, I. Taniguchi, and T. Onoye, "Duck Curve Aware Dynamic Pricing and Battery Scheduling Strategy Using Reinforcement Learning," *IEEE Transactions on Smart Grid*, vol. 15, no. 1, pp. 457–471, Jan. 2024, https://doi.org/10.1109/TSG.2023.3288355.

[12] A. Kaur, L. Nonnenmacher, and C. F. M. Coimbra, "Net load forecasting for high renewable energy penetration grids," *Energy*, vol. 114, pp. 1073–1084, Nov. 2016, https://doi.org/10.1016/j.energy.2016.08.067.

[13] L. Ai Wong and V. K. Ramachandaramurthy, "A Case Study on Optimal Sizing of Battery Energy Storage to Solve 'Duck Curve' Issues in Malaysia," in *2020 International Conference on Smart Grid and Clean Energy Technologies*, Kuching, Malaysia, 2020, pp. 1–4, https://doi.org/10.1109/ICSGCE49177.2020.9275649.

[14] Q. Hou, N. Zhang, E. Du, M. Miao, F. Peng, and C. Kang, "Probabilistic duck curve in high PV penetration power system: Concept, modeling, and empirical analysis in China," *Applied Energy*, vol. 242, pp. 205–215, May 2019, https://doi.org/10.1016/j.apenergy.2019.03.067.

[15] M. Sheha, K. Mohammadi, and K. Powell, "Solving the duck curve in a smart grid environment using a non-cooperative game theory and dynamic pricing profiles," *Energy Conversion and Management*, vol. 220, Sept. 2020, Art. no. 113102, https://doi.org/10.1016/j.enconman.2020.113102.

[16] J. Pei, N. Liu, J. Shi, and Y. Ding, "Tackling the duck curve in renewable power system: A multi-task learning model with iTransformer for net-load forecasting," *Energy Conversion and Management*, vol. 326, Feb. 2025, Art. no. 119442, https://doi.org/10.1016/j.enconman.2024.119442.

[17] R. Bowers, E. Fasching, and A. Antonio. "As solar capacity grows, duck curves are getting deeper in California." U.S. Energy Information Administration (EIA). https://www.eia.gov/todayinenergy/detail.php?id=56880.

[18] S. Wilkinson, M. J. Maticka, Y. Liu, and M. John, "The duck curve in a drying pond: The impact of rooftop PV on the Western Australian electricity market transition," *Utilities Policy*, vol. 71, Aug. 2021, Art. no. 101232, https://doi.org/10.1016/j.jup.2021.101232.

[19] Agora Energiewende, "Flexibility in thermal power plants: With a focus on existing coal-fired power plants," Berlin, Germany, 115/04-S-2017/EN, June 2017.

[20] D. Suri, J. de Chalendar, and I. M. L. Azevedo, "Assessing the real implications for CO_2 as generation from renewables increases," *Nature Communications*, vol. 16, no. 1, Aug. 2025, Art. no. 7124, https://doi.org/10.1038/s41467-025-59800-4.

[21] K. Li, H. Fan, and P. Yao, "Estimating carbon emissions from thermal power plants based on thermal characteristics," *International Journal of Applied Earth Observation and Geoinformation*, vol. 128, Apr. 2024, Art. no. 103768, https://doi.org/10.1016/j.jag.2024.103768.

[22] C. Gopal, M. Mohanraj, P. Chandramohan, and P. Chandrasekar, "Renewable energy source water pumping systems—A literature review," *Renewable and Sustainable Energy Reviews*, vol. 25, pp. 351–370, Sept. 2013, https://doi.org/10.1016/j.rser.2013.04.012.

[23] H. Hou, B. Xie, and Y. Cheng, "Analysis of Carbon Emissions and Emission Reduction from Coal-Fired Power Plants Based on Dual Carbon Targets," *Sustainability*, vol. 15, no. 9, Apr. 2023, Art. no. 7369, https://doi.org/10.3390/su15097369.

[24] M. J. B. Kabeyi and O. A. Olanrewaju, "Sustainable Energy Transition for Renewable and Low Carbon Grid Electricity Generation and Supply," *Frontiers in Energy Research*, vol. 9, Mar. 2022, Art. no. 743114, https://doi.org/10.3389/fenrg.2021.743114.

[25] H. W. Pandey, R. Kumar, and R. K. Mandal, "Ranking of mitigation strategies for duck curve in Indian active distribution network using MCDM," *International Journal of System Assurance Engineering and Management*, vol. 14, no. 4, pp. 1255–1275, Aug. 2023, https://doi.org/10.1007/s13198-023-01929-w.

[26] P. Julianto, "Unit Commitment Dengan Integrasi Pump Storage Hydroelectricity Untuk Mengatasi Masalah Duck Curve," *Elektrika Borneo*, vol. 8, no. 2, pp. 12–17, Nov. 2022, https://doi.org/10.35334/jeb.v8i2.3072.

[27] R. Wang, L. Zhang, C. Shi, and C. Zhao, "A Review of Gravity Energy Storage," *Energies*, vol. 18, no. 7, Apr. 2025, Art. no. 1812, https://doi.org/10.3390/en18071812.

[28] M. D'Auria *et al.*, "A Model of Integration between a CSP System and a PV Solar Field Sharing a Solid Particles Two-Tanks Thermal Storage," *Energies*, vol. 16, no. 22, Nov. 2023, Art. no. 7564, https://doi.org/10.3390/en16227564.

[29] J. D. Hunt *et al.*, "Existing and new arrangements of pumped-hydro storage plants," *Renewable and Sustainable Energy Reviews*, vol. 129, Sept. 2020, Art. no. 109914, https://doi.org/10.1016/j.rser.2020.109914.

[30] J. Kulpa, M. Kopacz, K. Stecuła, and P. Olczak, "Pumped Storage Hydropower as a Part of Energy Storage Systems in Poland—Młoty Case Study," *Energies*, vol. 17, no. 8, Apr. 2024, Art. no. 1830, https://doi.org/10.3390/en17081830.

[31] R. Mena, M. Godoy, C. Catalán, P. Viveros, and E. Zio, "Multi-objective two-stage stochastic unit commitment model for wind-integrated power systems: A compromise programming approach," *International Journal of Electrical Power & Energy Systems*, vol. 152, Oct. 2023, Art. no. 109214, https://doi.org/10.1016/j.ijepes.2023.109214.

[32] B. M. Hussein and A. S. Jaber, "Unit commitment based on modified firefly algorithm," *Measurement and Control*, vol. 53, no. 3–4, pp. 320–327, Mar. 2020, https://doi.org/10.1177/0020294019890630.

[33] H. Abdi, "Profit-based unit commitment problem: A review of models, methods, challenges, and future directions," *Renewable and Sustainable*

Energy Reviews, vol. 138, Mar. 2021, Art. no. 110504, https://doi.org/10.1016/j.rser.2020.110504.

[34] J. Li, J. Wen, and X. Han, "Low-carbon unit commitment with intensive wind power generation and carbon capture power plant," *Journal of Modern Power Systems and Clean Energy*, vol. 3, no. 1, pp. 63–71, Mar. 2015, https://doi.org/10.1007/s40565-014-0095-6.

[35] K. Aurangzeb, S. Shafiq, M. Alhussein, Pamir, N. Javaid, and M. Imran, "An effective solution to the optimal power flow problem using meta-heuristic algorithms," *Frontiers in Energy Research*, vol. 11, Sept. 2023, Art. no. 1170570, https://doi.org/10.3389/fenrg.2023.1170570.

[36] H. O. R. Howlader, M. M. Sediqi, A. M. Ibrahimi, and T. Senjyu, "Optimal Thermal Unit Commitment for Solving Duck Curve Problem by Introducing CSP, PSH and Demand Response," *IEEE Access*, vol. 6, pp. 4834–4844, 2018, https://doi.org/10.1109/ACCESS.2018.2790967.